Materials Physics and Mechanics 41 (2019) 1-7 Received: January 31, 2018

REDUCTION OF GRAPHENE FROM GRAPHENE OXIDE IN DIFFERENT MEDIA

V.A. Labunov, L.V. Tabulina*, I.V. Komissarov, L.A. Mikhnavets, A.N. Tkach

Belarusian State University of Informatics and Radioelectronics, Minsk, Belarus

*e-mail: Tabulina.Lyudmila@gmail.com

Abstract. Features of the reduction of graphene from graphene oxide in media containing hydrazine hydrate, ethylene glycol, and hydrogen are studied. X-ray energy dispersive spectroscopy, Raman spectroscopy, and scanning electron microscopy data indicate that this process proceeds through the high-temperature annealing of graphene oxide in a hydrogen environment.

Keywords: graphene, graphene oxide, Hummers method, nanostructure, reduction

1. Introdiction

Graphene is a material whose discovery was awarded with the 2010 Nobel Prize in physics. It is historically the first two-dimensional crystalline material whose properties differ appreciably from its three-dimensional structural analog, graphite. This thinnest of crystalline materials has a surprising combination of properties: transparency, mechanical strength, elasticity, exceptionally high mobility of charge carriers (massless Dirac fermions), and high thermal conductivity; it is elastic and impermeable to molecules of other substances. It is also more inert than gold when it comes to the effects of external conditions [1,2].

All of these characteristics, which are apparent in different physicochemical processes, make graphene a highly promising material for practical use in everything from nanoelectronics to composite materials [3]. This explains the enormous interest of physicists and chemists in synthesizing this exotic material, applications of which are impossible without the development of reliable and relatively inexpensive methods of preparation [4–6]. The best way of achieving this today is to use graphene oxide produced in the form of flakes by delaminating graphite with oxidizing reagents. This material can be considered graphite intercalated with oxygen-containing carbon groups that give it the ability to be thoroughly dispersed in water and hydrophilic organic solvents [7,8].

When interacting with chemical reducing reagents, graphene oxide is converted into thin graphene flakes of low structural quality [5–7] due to the substantial degradation of graphite during the synthesis of graphene oxide. Nevertheless, graphene can be prepared from this material [6–10]. These data are, however, difficult to compare, since reagents that differed in their chemical properties were used, and the processes involving them were performed under different thermal conditions. In addition, graphite materials of different structural quality and fineness were used to obtain graphene oxide [6,7,10]. In this work, we studied the effects of reducing agents used in [4,7–10] had on the structure and chemical composition of graphene oxide in order to assess the prospects for using it for obtaining graphene. In all reduction processes, graphene oxide was prepared from graphite with the same chemical composition, structure, and grain size. Such research methods as X-ray energy dispersive spectroscopy (XEDS), Raman spectroscopy, and scanning electron microscopy

http://dx.doi.org/10.18720/MPM.4112019_1

(SEM) were used to assess the quantitative and qualitative compositions of the initial and final materials, and their structural features.

2. Experimental

Table 1 presents data on quantitative and qualitative compositions of the materials and the corresponding specific surface areas. Analysis of the data of Table 1 indicates that the C/O atomic ratio of graphene oxide differs significantly from that of the original graphite (Table 1, methods 1 and 2) and coincides with the ones presented in [5,8,9]. In addition, the mass distributions of oxygen in the graphene oxide arrays and materials obtained with methods 1 and 2 have considerable heterogeneity (±4.1 wt %). This is probably because of the nonuniform thickness of the graphene oxide flakes that formed and the nonuniform distribution of water molecules, hydroxyl (OH), carboxyl (COOH), carbonyl (CHO), and epoxy (C–O–C) groups in their conglomerates. The above testifies to the different thickness of graphite delamination during the formation of graphene oxide using the Hummers technique and the weak impact reduction methods 1 and 2 had on this factor.

Table 1. Qualitative and quantitative composition of materials and their specific surface areas

	[C], wt %	[O], wt %	[Fe], wt %	[S], wt %	[P], wt %	[Mn], wt %	C/O	*S*, m^2/g
1	92.8 ± 0.6	1.7 ± 0.3	0.05	0.00	0.00	0.00	66.1±3.9	11
2	57.8 ± 6.2	39.7 ± 4.1	0.00	0.90 ± 0.10	0.2±0.1	1.00 +0.00	1.9±0.2	53
3	69.5 ± 6.3	27.8 ± 4.1	0.00	0.50 ± 0.10	0.2±0.1	0.00	3.3±0.1	57
4	67.1 ± 6.1	31.0 ± 4.1	0.00	0.60 ± 0.10	0.1±0.0	0.00	2.8±0.1	54
5	78.4 ± 3.6	18.0 ± 1.6	0.00	0.08 ± 0.05	0.1±0.0	0.00	5.7±0.1	124
6	88.1 ± 0.5	5.5 ± 0.3	0.00	0.08 ± 0.05	0.1±0.0	0.00	21.0±0.4	258

(1) Crushed graphite; (2) graphene oxide; (3) after reduction with method 1; (4) after reduction with method 2; (5) after reduction with method 3; and (6) after reduction with method 4. C/O is the atomic ratio and S is the surface area.

A comparison of C/O atomic ratios of graphene oxide and the materials obtained using methods 1–4 indicates that the latter had higher values. The substances obtained with methods 3 and 4 and subjected to annealing in an Ar/H_2 environment have the greatest values. The annealing of graphene oxide at 200 and 1000°C in particular increased the C/O atomic ratio value by factors of ≈3 and 11, respectively (Table 1, methods 2, 5, and 6). When methods 1 and 2 were used for the reduction of graphene oxide, the greatest change in the C/O atomic ratios in its bulk was for method 1, i.e., in hydrazine hydrate. The initial C/O atomic ratio in this case grew by a factor of ≈1.8.

Table 2. Characteristics of the materials' Raman spectra peaks

No	Frequency, cm^{-1}			Relative intensity		
	D	G	2D	I_D/I_G	I_{2D}/I_G	I_{2D}/I_D
1	1349	1579	2700	0.24	0.50	2.1
2	1352	1586	2658	1.06	0.03	0.03
3	1350	1583	2685	1.02	0.09	0.08
4	1349	1586	2685	1.09	0.09	0.08
5	1340	1583	2679	1.50	0.08	0.06
6	1344	1580	2675	0.94	0.24	0.26

The notation is the same as in Table 1.

The data of Table 1 also indicate that graphene oxide contains small residual amounts of the reactants used in its synthesis. In particular, it contains ≈0.3% of phosphorus, 1.0% of sulfur, and 1.0% of manganese. The chemical composition of the materials obtained by methods 1–4 are of high purity, especially in the case of methods 3 and 4. The latter materials contained 0.1% phosphorus, sulfur impurities more than an order of magnitude less than those of graphene oxide, and no manganese compounds (Table 1, methods 2–6). Overall, these data show that graphene oxide and the materials prepared by its reduction by methods 1–4 had almost no inorganic impurities.

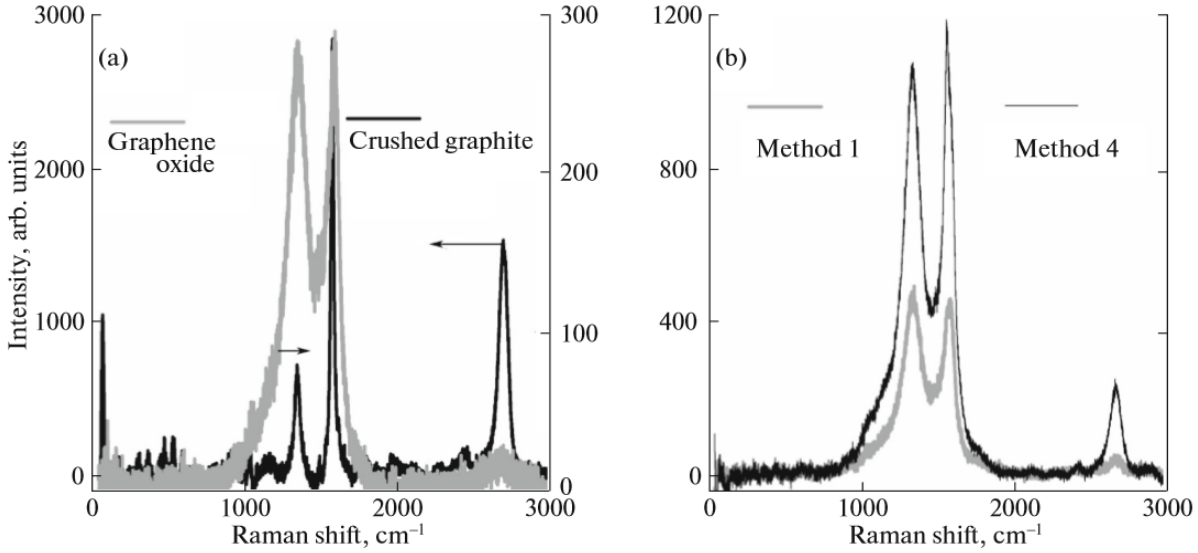

Fig. 1. Raman spectra of (a) crushed graphite and graphene oxide, and (b) materials obtained from graphene oxide via reduction in hydrazine hydrate (method 1) and Ar/H_2 at 1000°C (method 4). Arrows show the axis of intensity

The specific surface areas of the initial crushed graphite and that of graphene oxide (Table 1) were 11 and 53 m^2/g, respectively. The specific surface areas of the substances obtained by methods 1 and 2 are almost the same as those of graphene oxide (Table 1, methods 1–4). The materials formed by methods 3 and 4, however, had greater specific surface areas and grew by ≈ 500% after treatment by method 4 (Table 1, methods 2, 5, and 6). The structure of graphene oxide was probably subjected to additional delamination processes during annealing, especially under high temperature conditions.

It should be noted that the specific surface areas of graphene oxide and the materials obtained with methods 1–4 were considerably smaller than those observed in [4,10,14]. We may assume this was due to the aggregation of flakes upon drying into conglomerates that contained micropores. There could be volumetric filling by the adsorbate (nitrogen) during adsorption measurements [15], or they might be filled with physically adsorbed water, molecules of which inside the cavities of micropores are grouped into strong energy-stable clusters [16]. The first factor leads to larger surface areas of the materials, while the second results in the smaller sizes observed in this work (Table 1, methods 2–6). This indicates that using adsorption and the BET equation to estimate the specific surfaces of the graphene material can produce values that have no physical meaning, as was noted in [10].

The Raman spectra of the investigated materials are presented in Table 2 and Fig.1. They contain the D, G, and 2D bands at 1350, 1580, and 2700 cm^{-1}, respectively that are characteristic of graphene structures. The D band is due to some amorphous phase or cleaved sp^2 carbon bonds in the carbon rings of graphene structures (cleaved bonds at the edges of

graphene conglomerates and the emergence of sp3 carbon bonds). The G band is due to sp^2 carbon bonds in the dense hexagonal graphene structures. The shape, position, and intensity of the 2D band are sensitive to the quality of carbon rings in the graphene layers and their number when it is 5 [6,7,11].

The frequencies of bands D, G, and 2D of the investigated materials and intensity ratios I_D/I_G, I_{2D}/I_G, and I_{2D}/I_D, a measure of disorder in graphene layers [7,11], are given in Table 2. At the same time, the high I_D/I_G and low I_{2D}/I_G and I_{2D}/I_D values indicate a higher degree of defectiveness for the graphene materials. Analysis of these data shows that graphene oxide had substantially higher I_D/I_G and lower I_{2D}/I_G and I_{2D}/I_D values than the crushed initial graphite. This indicates there were a great many cleaved sp^2 carbon bonds in its structure [6–8,10,11]. The frequency shift of the G band toward the high-frequency region also indicates considerable defectiveness of the graphene oxide structure (Table 2, methods 1, 2) [7].

The above is also typical of the materials obtained from graphene oxide by the methods 1–3 (see Table 2, methods 1, 3–5), where there was a large number of oxygen-containing groups (Table 1). In addition, the I_D/I_G, I_{2D}/I_G, and I_{2D}/I_D values of graphene oxide formed by the method 3 (i.e., obtained in an Ar/H_2 environment at 200°C) testify to its high structural defectiveness. This is probably because there was additional delamination of graphene oxide flakes under these conditions, but the effect hydrogen reduction had on their structure was slight. The high-temperature annealing of the material in the same medium (method 4), however, not only lowers the number of oxygen-containing groups in its flakes considerably, as can be seen from Table 1; it greatly improves their graphene structure. This is confirmed by the changes in the corresponding I_D/I_G, I_{2D}/I_G, and I_{2D}/I_D values on the Raman spectra of the materials obtained with methods 1–4 (Table 2, methods 2–6). In addition, the 2D band maximum in the Raman spectrum of the substance obtained with method 4 was observed at 2675 cm^{-1} (Table 2, method 6), which is typical for single-layer graphene [17].

The shapes of the 2D bands in the Raman spectra (Fig. 1) also illustrate a different quality of the structure of graphene layers in materials 1–3 and 6 (Table 2). The 2D band in the Raman spectrum of the initial crushed graphite (Fig. 1a) is intense and narrow, but does not contain a 2D2 curve in the low frequency region. This indicates initial three-dimensional disorder of the graphene layers in this material [7], due probably to its grinding. The 2D band in the Raman spectrum of graphene oxide is not only of low intensity; it broadens due to the high structural defectiveness of carbon rings in flakes of this material [7,9]. As a result, there is a strong superpositioning of bands D and G.

A considerable overlap of bands D and G was also observed in the Raman spectrum of the material obtained by method 1. The corresponding 2D band is not intense, but it is narrower (Figs. 1b), indicating some slight reductive transformation of the graphene oxide structure. If we compare the shapes of 2D bands in the Raman spectra of the materials obtained by the methods 1 and 4, however, the band of the latter material is much narrower and more intense. Nevertheless, if we compare the 2D bands of this material and graphene obtained micro-mechanically [11], the band of the reduced graphene is broader and less intense. This indicates that monolayer graphene flakes formed by treating graphene oxide by method 4, but their structure is more defective than that of graphene obtained using the micromechanical approach. We may assume that the different shapes of the 2D bands in the Raman spectra of these materials are due to the formation of graphene flakes during the high-temperature annealing of graphene oxide in an Ar/H_2 medium with a wide distribution of their areas.

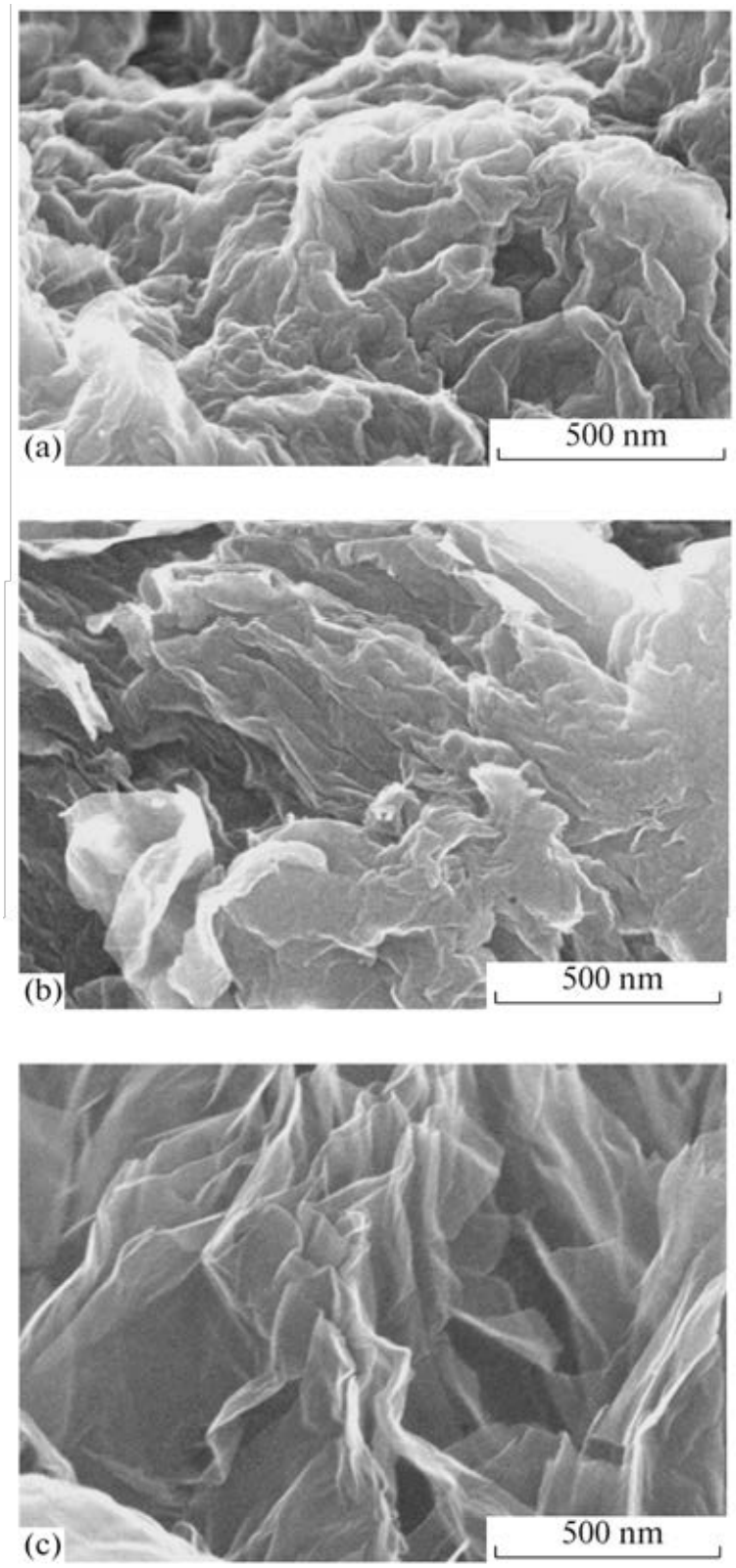

Fig. 2. SEM images of (a) graphene oxide, (b, c) materials obtained from graphene oxide via reduction in hydrazine hydrate (method 1) and Ar/H_2 at 1000°C (method 4), respectively

Figure 2 shows SEM images of graphene oxide and the materials obtained by the methods 1 and 4. They indicate that morphology of conglomerates in graphene oxide has great relief in which flakes are tightly grouped (Fig. 2a). The structure of the resulting

conglomerates in the material processed by the method 1 is almost similar to that of graphene oxide (Fig. 2b), but conglomerates of the material obtained by method 4 are much looser. In contrast to graphene oxide, the flakes in this material are somewhat affected by strong Van der Waals bonds during aggregation, due to the low number of oxygen-containing structural groups.

3. Conclusions

Our study of features of the reduction of graphene oxide from graphene at different temperatures and in various media indicates that this process is proceeds only upon high-temperature annealing in an inert atmosphere containing hydrogen. This results in [18,19] complete removal of physically adsorbed water from the micropores in a graphene oxide and contributes to the destruction of mobile oxygen-containing carbon groups in the structure of flakes, generally enhancing the effect of hydrogen reduction on them. This leads to dramatic changes in the chemical composition and structure of this material, producing single-layer graphene flakes.

Acknowledgements. *The authors are grateful to their colleagues at NTTs Belmikrosistemy for their support in studying the materials used in this work.*

References

[1] Geim AK. Nobel Lecture: Random walk to graphene. *Reviews of Modern Physics.* 2011;83(3): 851-862.

[2] Novoselov KS. Nobel lecture: Graphene: materials in the flatland. *Reviews of Modern Physics*. 2011;83(3): 837-849.

[3] Sorokin PB, Chernozatonskii LA. Graphene-based semiconductor nanostructures. *Physics-Uspekhi.* 2013;56(2): 105-122.

[4] Stankovich S, Dikin DA, Piner RD, Kohlhaas KA, Kleinhammes A, Jia Y, Wu Y, Nguyen ST, Ruoff RS. Synthesis of graphene-based nanosheets via chemical reduction of exfoliated graphite oxide. *Carbon.* 2007;45(7): 1558-1565.

[5] Novikov VP, Kirik SA. Low-temperature synthesis of graphene. *Technical Physics Letters.* 2011;37(6): 565-567.

[6] Tkachev SV, Buslaeva EY, Naumkin AV, Kotova SL, Laure IV, Gubin SP. *Inorganic Materials*. 2012;48(8): 796-802.

[7] Kaniyoor A, Ramaprabhu S. A Raman spectroscopic investigation of graphite oxide derived graphene. *AIP Advances.* 2012;2(3): 032181.

[8] Marcano DC, Kosynkin DV, Berlin JM. Improved synthesis of graphene oxide. *ACS Nano.* 2010;4(8): 4806-4814.

[9] Watcharotone S, Dikin DA, Stankovich S, Piner RD, Jung I, Dommet GH, Evmenenko G, Wu SE, Chen SF, Liu CP, Nguyen ST, Ruoff RS. Graphene-silica composite thin films as transparent conductors. *Nano Letters*. 2007;7(7): 1888-1892.

[10] Hsieh CT, Hsu SM, Lin JY. Fabrication of graphene-based electrochemical capacitors. *Japanese Journal of Applied Physics*. 2012;51(1): 01AH06.

[11] Some S, Kim Y, Yoon Y, Yoo HJ, Lee S, Park Y, Lee H. High-quality reduced graphene oxide by a dual-function chemical reduction and healing process. *Scientific Reports.* 2013;3: 1929.

[12] Shulitskii BG, Tabulina LV, Rusal'skaya TG, Shaman YP, Komissarov I, Karoza AG. Effect of the multistage chemical treatment of carbon nanotubes on their purity and quality of walls. *Russian Journal of Physical Chemistry A.* 2012;86(10): 1595-1601.

[13] Gregg SJ, Sing KSW. *Adsorption, Surface Area, and Porosity.* London: Academic; 1967.

[14] Zhu Y, Murali S, Cai W, Li X, Suk JW, Potts JR, Ruoff RS. Graphene and graphene oxide: synthesis, properties, and applications. *Advanced Materials*. 2010;22(35): 3906-3924.
[15] Dubinin MM, Serpinskii VV. (Eds.) *Proceedings of the 4th All-Union Conference on Theoretical Problems of Adsorption.* Moscow: Nauka; 1976. (in-Russian)
[16] Kadlets O. *Adsorption in Micropores.* Moscow: Nauka; 1983.
[17] Costa SD, Righi A, Fantini C, Hao Y, Magnuson C, Colombo L, Ruoff RS, Pimenta MA. Resonant Raman spectroscopy of graphene grown on copper substrates. *Solid State Communications.* 2012;152(15): 1317-1320.
[18] Ganguly A, Sarma S, Papakonstantinou P, Hamilton J. Probing the thermal deoxygenation of graphene oxide using high-resolution in situ X-ray-based spectroscopies. *Journal of Physical Chemistry C*. 2011;115(34): 17009-17019.
[19] Zavilopulo AN, Mykyta MI, Shpenik OB. Mass-spectrometric investigation of coal gases from samples with a low and high degree of coalification. *Technical Physics.* 2012;57(7): 923-930.